ALLUVIAL CHANNEL GEOMETRY: THEORY AND APPLICATIONS

By Pierre Y. Julien, Member, ASCE,[1] and Jayamurni Wargadalam[2]

ABSTRACT: The downstream hydraulic geometry of alluvial channels, in terms of bank-full width, average flow depth, mean flow velocity, and friction slope, is examined from a three-dimensional stability analysis of noncohesive particles under two-dimensional flows. Four governing equations (flow rate, resistance to flow, secondary flow, and particle mobility) are solved to analytically define the downstream hydraulic geometry of noncohesive alluvial channels as a function of water discharge, sediment size, Shields number, and streamline deviation angle. The exponents of hydraulic geometry relationships change with relative submergence. Four exponent diagrams illustrate the good agreement with several empirical regime equations found in the literature. The analytical formulations were tested with a comprehensive data set consisting of 835 field channels and 45 laboratory channels. The data set covers a wide range of flow conditions from meandering to braided, sand-bed and gravel-bed rivers with flow depths and channel widths varying by four orders of magnitude. Figures illustrate the results of the three-part analysis consisting of calibration, verification, and validation of the proposed hydraulic geometry equations. Field and laboratory observations are in very good agreement with the calculations of flow depth, channel width, mean flow velocity, and friction slope.

INTRODUCTION

Deformable alluvial channels are known to adjust their slope, width, depth, and velocity to achieve stable conditions at a specified supply of water and sediment. Downstream hydraulic geometry relationships describe the shape of bank-full alluvial channels in terms of bank-full width, average flow depth, average flow velocity, and channel slope. Considerable progress has been achieved in river mechanics after a century of field investigations on the geometry of alluvial rivers under equilibrium, or in regime. Primary contributions include those of Kennedy (1895), Lindley (1919), Lacey (1929), Lane (1937), Leopold and Maddock (1953), Mahmood and Shen (1971), and Blench (1969, 1972). Simons and Albertson (1963) delineated several channel conditions, and their graphical relationships were later supported by Henderson (1966). From dimensional analysis and physical reasoning, several authors, including Chien (1957), Henderson (1961), Stebbins (1963), and Gill (1968), presented physical support for the regime equations. Parker (1978) investigated self-formed straight rivers with equilibrium banks and mobile bed for sand-silt and gravel-bed rivers. He obtained rational regime equations from the concept of lateral transfer of downstream momentum by turbulent diffusion. Comprehensive reviews of the abundant literature on the regime approach and other methods defining the downstream hydraulic geometry relationships are available in Chitale (1973), Callander (1978), Engelund and Fredsoe (1982), Ranga Raju and Garde (1988), and Yalin (1992). Limitations of most existing methods relate to the simplified one-dimensional (1D) analyses of flow and sediment transport in alluvial channels.

Two-dimensional (2D) flows are not only important to define flow patterns in meandering and braiding channels, but also to determine the particle migration rate and the rate of alluvial channel deformation and, thus, the hydraulic geometry of alluvial channels.

This study extends earlier contributions by Julien (1988, 1989); the primary objective is to analytically define the equilibrium downstream hydraulic geometry relationships of deformable alluvial channels. The innovative aspects of this study include the concepts of secondary flows in curved channels, and the three-dimensional (3D) mobility of noncohesive particles. Downstream hydraulic geometry equations are theoretically derived and the variability of the exponents is examined through exponent diagrams. Practical applications are obtained after an extensive calibration, verification, and validation of simplified hydraulic geometry relationships with a data set of 835 rivers and channels.

[1]Assoc. Prof., Dept. of Civ. Engrg., Engrg. Res. Ctr., Colorado State Univ., Ft. Collins, CO 80523.
[2]Grad. Student, Dept. of Civ. Engrg., Colorado State Univ., Fort Collins, CO.

Note. Discussion open until September 1, 1995. To extend the closing date one month, a written request must be filed with the ASCE Manager of Journals. The manuscript for this paper was submitted for review and possible publication on October 14, 1993. This paper is part of the ***Journal of Hydraulic Engineering***, Vol. 121, No. 4, April, 1995. ©ASCE, ISSN 0733-9429/95/0004-0312-0325/$2.00 + $.25 per page. Paper No. 7171.

FLOW CHARACTERISTICS IN ALLUVIAL CHANNELS

The downstream hydraulic geometry—regime geometry—of noncohesive alluvial channels can be determined from the stability of sediment particles under 2D flow conditions. The downstream hydraulic geometry is defined in terms of surface channel width W, average flow depth h, average flow velocity $\bar{U}$, and channel slope S.

Under steady uniform bank-full flow conditions, the dominant discharge Q is

$$Q = Wh\bar{U} \tag{1}$$

where the mean velocity vector $\bar{U}$ is taken normal to the cross-sectional area.

Flow resistance in alluvial channels is quite complex as proved by Simons and Senturk (1977). When considering turbulent flows over hydraulically rough boundaries of sediment size d_s, the logarithmic resistance relationship proposed by Keulegan (1938) describes grain roughness

$$\frac{1}{\sqrt{f}} = a \ln\left(\frac{12.2h}{d_s}\right) \tag{2}$$

where the Darcy-Weisbach friction factor f is written as a function of the relative submergence h/d_s, and gravitational acceleration g. Because the logarithmic form of the resistance equation is not conducive to closed-form solutions, the following equivalent power form is preferred:

$$\frac{1}{\sqrt{f}} = b\left(\frac{h}{d_s}\right)^m \tag{3}$$

where the value of the exponent m, which defines the slope of the tangent to the semilogarithmic resistance formula (2), on the log-log paper, is the following function of the relative submergence h/d_s:

$$m = \frac{1}{\ln\left(\frac{12.2h}{d_s}\right)} \tag{4}$$

As the relative submergence h/d_s becomes increasingly large, the exponent m reduces to zero ($m \to 0$, when $h/d_s \to \infty$). In this case, both the Darcy-Weisbach friction factor f and the Chezy coefficient C remain constant because $f = 8g/C^2$. For intermediate values of relative submergence $h/d_s = 200$, the well-known Manning-Strickler relationship ($m = 1/6$) is comparable to the logarithmic equation.

In channels with coarse bed materials, the exponent m increases rapidly at low values of relative submergence ($h/d_s < 10$). This is corroborated by the following empirical results: Leopold and Wolman (1957) found $m = 0.5$, when $0.7 < h/d_s < 10$; Ackers (1964) proposed $m = 0.25$, when $3 < h/d_s < 13$; Kellerhals (1967) suggested $m = 0.25$; Charlton et al. (1978) recommended $m = 0.44$, when $2 < h/d_{90} < 10$; Bray (1979) found $m = 0.281$ in gravel-bed streams; and Mussetter (1989) suggested $m = 0.46$, when $0.2 < h/d_{84} < 4$ for very steep cobble and boulder-bed streams.

Thus, the average flow velocity follows from (3) as proposed by Einstein and Chien (1954)

$$\bar{U} = b\sqrt{8g}\left(\frac{h}{d_s}\right)^m h^{1/2}S^{1/2} \tag{5}$$

where the exponent m increases with decreasing relative submergence.

The downstream bed shear stress τ_θ applied in straight open channels under steady uniform flow conditions is a function of the bed slope S, the mass density of water ρ, and the hydraulic radius $R_h = Kh$

$$\tau_\theta = K\rho ghS \tag{6}$$

For channels with large width-depth ratios, the parameter K approaches unity and the hydraulic radius R_h becomes equal to the flow depth h.

Two-Dimensional Flow in Alluvial Channels

Secondary circulation in curved channels is generated through a change in downstream channel orientation. The streamlines near the surface are deflected toward the outer bank, whereas those near the bed are deviated toward the inner bank. The near-bed velocity, the tangential bed shear stress, and the drag on the bed particles are commonly directed toward the inner bank.

Flow in bends is analyzed in cylindrical coordinates. The relative magnitude of radial acceleration terms indicates that the centrifugal acceleration is counterbalanced by pressure gradient and radial shear stress, as suggested by Rozovskii (1961)

$$\frac{u^2}{r} = gS_r - \frac{1}{\rho}\frac{\partial \tau_r}{\partial z} \tag{7}$$

where the local downstream velocity u, the radial shear stress τ_r, and the radial water surface slope S_r vary with the vertical elevation z and/or the radius of curvature r. In Fig. 1, the transverse boundary shear stress τ_{rR} at point R_A, the radial water surface slope S_{rA} at point A, the radius of curvature R at the same point, the average flow depth h, and the top channel width W serve as scaling factors. These scaling factors define dimensionless parameters for channel width $w^* = w/W$; flow depth $z^* = z/h$; radius of curvature $r^* = r/R$; velocity $u^* = u/\tilde{U}$; radial shear stress $\tau_r^* = \tau_r/\tau_{rR}$; and the radial surface slope $S_r^* = S_r/S_{rA}$. The element of fluid volume $d\forall = ds\, dz\, dw$ for a reach of given length ds is reduced to a dimensionless volume $d\forall^* = d\forall/WRh$. The radial equation of motion (7) is multiplied by ρ and $d\forall$, reduced in dimensionless form, and then integrated over the dimensionless volume $\forall^*$ of the reach. The resulting dimensionless momentum equation in the radial direction is

$$\rho Wh\tilde{U}^2 \int_{\forall^*} \frac{u^{*2}}{r^*}\, d\forall^* = \rho gRWhS_{rA} \int_{\forall^*} S_r^*\, d\forall^* - RW\tau_{rR} \int_{\forall^*} \frac{\partial \tau_r^*}{\partial z^*}\, d\forall^* \tag{8}$$

The corresponding force diagram is shown in Fig. 1 after denoting the centrifugal force on the left-hand side of (8) by F_c, while the pressure force F_p describes the first term on the right-hand side of (8), and the last integral in (8) represents the shear force F_s. The pressure force is found to balance the sum of the centrifugal force exerted at a distance c above point A, while the shear force is exerted at a distance d below point A. The moment equilibrium around point A results in

$$\Omega_r = \frac{\rho h\tilde{U}^2}{R\tau_{rR}} = \frac{d\displaystyle\int_{\forall^*} \frac{\partial \tau_r^*}{\partial z^*}\, d\forall^*}{c\displaystyle\int_{\forall^*} \frac{u^{*2}}{r^*}\, d\forall^*} \tag{9}$$

The dimensionless parameter Ω_r = ratio of the centrifugal force generating secondary motion to the shear force abating the motion and dissipating energy. The resulting ratio of radial shear stress τ_{rR} to the downstream bed shear stress τ_θ defines the deviation angle λ of the streamlines near the bed. Therefore

$$\tan \lambda = \frac{\tau_{rR}}{\tau_\theta} = D\frac{h}{R} \tag{10}$$

where parameter $D = (8b^2/K\Omega_r)(h/d_s)^{2m}$ is obtained from combining (5), (6), and (9).

Slightly different values of D were proposed by Rozovskii (1961), Engelund (1974), Zimmermann (1977), de Vriend (1977), Odgaard (1981), Dietrich and Smith (1984), and Hussein and Smith (1986). The parameter D varies with relative submergence h/d_s around $D \approx 11$. The following formulation for the deviation angle λ is used, in which the values of p and b_r accommodate a wide spectrum of conditions pertaining to the secondary circulation in alluvial channel bends. For example, Rozovskii's (1961) approximation

$$\tan \lambda = b_r \left(\frac{h}{d_s}\right)^p \frac{h}{R} \tag{11}$$

corresponds with $D = 11$ when $b_r = 11$ and $p = 0$. Similarly, the theoretical relationship from combining (5), (6), (9), and (10) corresponds with $D = (8b^2/K\Omega_r)(h/d_s)^{2m}$ when $b_r = 8b^2/K\Omega_r$ and $p = 2m$.

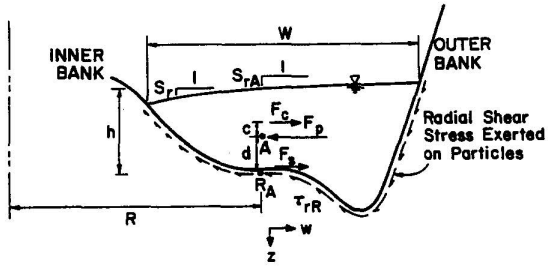

FIG. 1. Force Diagram for Flow in Curved Channels

PARTICLE STABILITY ANALYSIS IN ALLUVIAL CHANNELS

The stability of noncohesive particles in straight alluvial channels is described by the relative magnitude of the downstream shear force and the weight of the particle. The ratio of these two forces defines the longitudinal mobility factor, also called the Shields number τ_θ^*

$$\tau_\theta^* = \frac{\tau_\theta}{(\rho_s - \rho)gd_s} \tag{12}$$

where ρ_s = mass density of sediment particles. The critical value of the Shields number, $\tau_{\theta c}^* \approx 0.047$, identifies the beginning of motion of noncohesive particles in turbulent flows over rough boundaries. For values of the Shields number below the critical value ($\tau_\theta^* \leq \tau_{\theta c}^*$), the particles on the wetted perimeter of the alluvial channel are stable. Beyond this threshold ($\tau_\theta^* > \tau_{\theta c}^*$), the particles enter motion and the rate of sediment transport increases with the Shields number. Two significant concepts are associated with the Shields number: (1) the threshold concept described by $\tau_{\theta c}^*$ for the beginning of motion of noncohesive particles; and (2) the concept that beyond the threshold value, the sediment transport rate increases with the Shields number. Since the Shields number depends primarily on flow depth, it is associated with the vertical processes of aggradation and degradation in alluvial channels.

In straight alluvial channels without secondary circulation, a cross section is stable when threshold conditions exist simultaneously for all particles located on the channel's wetted perimeter. Lane (1955) solved this problem and found a cosinusoidal cross-sectional shape in which the flow depth is determined from the critical Shields number $\tau_{\theta c}^*$, and the bank slopes at the free surface are inclined at the submerged angle of repose ϕ.

Three-Dimensional Particle Stability Analysis

Flow in curved alluvial channels induces streamline deviations from the downstream direction, and a 3D stability analysis for particles along the wetted perimeter of the channel is required. The 3D analysis of Stevens and Simons (1971) considers both the lift force F_l and the drag force F_d applied on a particle of weight W_p and angle of repose ϕ on an embankment slope θ, given the near-bed streamline deviation angle λ. The buoyancy force on the particle, F_b, is subtracted from the particle weight to define the submerged particle weight W_s. In Fig. 2 the lift force F_l is acting in the direction normal to the embankment plane, and the drag force F_d is acting along the same plane in the direction of the velocity field near the particle. Near the bed, streamline deviations from the downstream direction are denoted by the deviation angle λ shown in Fig. 2. The stability against the rotation of sediment particles is determined from the sum of moments exerted against the point of rotation. From the Stevens and Simons (1971) analysis, a stability factor Ψ expresses the ratio of the resisting moment to the moment generating motion:

$$\Psi = \frac{\cos\theta \tan\phi}{\eta' \tan\phi + \sin\theta \cos\beta} \tag{13}$$

where the particle motion angle β, shown in Fig. 2, is calculated from

$$\beta = \tan^{-1}\left(\frac{\cos\lambda}{\frac{2\sin\theta}{\tan\phi} + \sin\lambda}\right) \tag{14}$$

and the modified critical Shields number η'

$$\eta' = 10.5\tau_{\theta c}^*(1 + \sin(\lambda + \beta)) \tag{15}$$

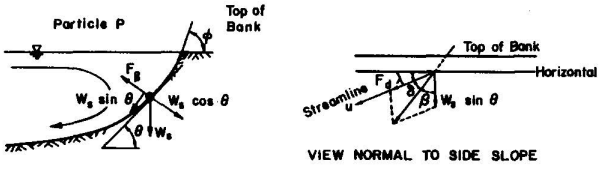

FIG. 2. Three-Dimensional Particle Stability Diagram

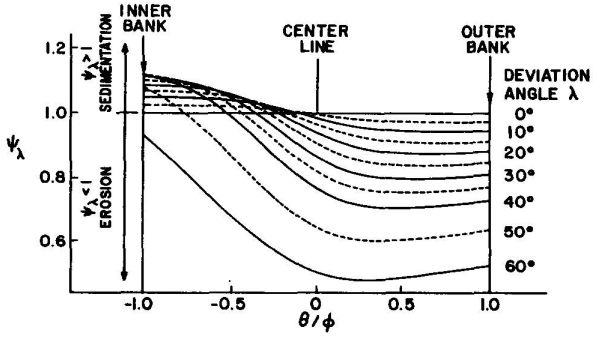

FIG. 3. Relative Stability of Sediment Particles in Curved Channels

Values of $\Psi = 1$ indicate threshold between stable condition ($\Psi > 1$) and particle motion ($\Psi < 1$). The cross-sectional geometry of a stable straight alluvial channel can be determined from (13)–(15) when $\lambda = 0$. This cross-sectional shape is similar to the cosinusoidal geometry defined by Lane (1955).

In curved channels, secondary flow effects are examined through the influence of the deviation angle λ on the values of the stability factor Ψ. Stability calculations based on (13)–(15), with $\lambda \neq 0$, demonstrate the slight downward deviations generated particle motion, while small upward deviations increase particle stability. On the other hand, particles under large upward deviations enter motion and cause erosion of the bed material.

Quantitative dimensionless results are summarized in Fig. 3 for typical 2D flow conditions in a curved alluvial channel. The local cross-sectional shape is described as the ratio of the embankment slope θ to the angle of repose ϕ. This figure illustrates the relative particle stability ratio $\Psi_\lambda = \Psi(\lambda \neq 0)/\Psi(\lambda = 0)$ of the stability factor with secondary circulation ($\lambda \neq 0$) over the stability factor without secondary circulation ($\lambda = 0$). Fig 3 shows that when the deviation angle λ is relatively small (e.g., less than 15°), the downward deflected streamlines near the outer bank ($\theta/\phi > 0$) induce particle motion, as expected from $\Psi_\lambda < 1$. Conversely, opposite effects are observed near the inner bank ($\theta/\phi < 0$); the upward deviations of the streamlines increase the stability of particles as portrayed by the values of $\Psi_\lambda > 1$. The conditions induced by secondary circulation at angles $\lambda < 15°$ are favorable to erosion near the outer bank and sedimentation near the inner bank of curved alluvial channels.

When the strength of secondary circulation increases, $15° < \lambda < 55°$, asymmetry in the particle stability curves develop, as shown in Fig. 3, and a larger proportion of the channel becomes unstable. For extreme conditions ($\lambda > 55°$), the entire cross section becomes unstable and scour occurs for all particles on the wetted perimeter of the alluvial channel, widening the channel.

This analysis of secondary circulation effects on particle mobility in curved alluvial channels highlights a continuum of conditions between the following two extremes: (1) At small deviation angles, around $\lambda < 15°$, equilibrium prevails between outer-bank erosion and inner-bank deposition; and (2) at large deviation angles, typically when $\lambda > 55°$, the imbalance between the erosion rate that exceeds the deposition rate causes widening of the alluvial channel. Secondary circulation effects being primarily felt near the outer bank, the deviation angle λ relates to the widening process in alluvial channels.

DOWNSTREAM HYDRAULIC GEOMETRY EQUATIONS

The downstream hydraulic geometry relationships for noncohesive alluvial channels under hydraulically rough turbulent flows are derived by combining the following four fundamental relationships: (1) Flow rate [(1)]; (2) resistance to flow [(5)]; (3) particle mobility [(12 and 6)]; and (4) secondary flow [(11)]. These four equations are combined and solved for channel width W, flow depth h, average flow velocity $\bar{U}$, and slope S, and are written as a power function of discharge Q, sediment size d_s, Shields parameter τ_θ^*, and deviation angle λ. The resulting equilibrium hydraulic geometry equations are

$$h = \alpha^{1/(2+m+p)} Q^{1/(2+m+p)} d_s^{(-1+2m+2p)/(4+2m+2p)} \tau_\theta^{*\,-1/(4+2m+2p)} (\tan\lambda)^{1/(2+m+p)} \tag{16}$$

$$W = \frac{b_r}{R_w} \alpha^{(1+p)/(2+m+p)} Q^{(1+p)/(2+m+p)} d_s^{(-1+2m-3p)/(4+2m+2p)} \tau_\theta^{*(-1-p)/(4+2m+2p)} (\tan\lambda)^{(-1-m)/(2+m+p)} \tag{17}$$

$$\bar{U} = \frac{R_w}{b_r} \alpha^{(-2-p)/(2+m+p)} Q^{m/(2+m+p)} d_s^{(2-4m+p)/(4+2m+2p)} \tau_\theta^{*(2+p)/(4+2m+2p)} (\tan\lambda)^{m/(2+m+p)} \tag{18}$$

$$S = \rho^* \alpha^{-1/(2+m+p)} Q^{-1/(2+m+p)} d_s^{5/(4+2m+2p)} \tau_\theta^{*(5+2m+2p)/(4+2m+2p)} (\tan\lambda)^{1/(2+m+p)} \tag{19}$$

where m and p = exponents defined in (5) and (11), respectively; $R_w = R/W$ = ratio of radius of curvature to channel width; $\rho^* = (\rho_s - \rho)/\rho K$ = dimensionless submerged mass density of the sediment; parameter α, defined as $\alpha = R_w/b_r b\sqrt{8g\rho^*}$, has the fundamental dimensions of $T/\sqrt{L}$.

Singularities of the system of equations, such as $\lambda = 0$ or $R_w = \infty$, are not relevant to this analysis because the hydraulic geometry of straight channels has already been defined by Lane (1955). It must also be considered that even in straight channels, the formation of alternate bars induces streamline deviations [Engelund and Skovgaard (1973), Parker (1976), Fredsoe (1978), Ikeda et al. 1981)], supporting the analyses based on $\lambda \neq 0$, and $R_w \neq \infty$.

QUALITATIVE ANALYSIS OF HYDRAULIC GEOMETRY EQUATIONS

A plethora of hydraulic geometry relationships is available in the literature. Typically, the channel width, depth, velocity, and slope are described in terms of bank-full discharge, dominant

discharge, and mean annual discharge in either the SI or English system of units. Fewer relationships include sediment size as a second variable, and reference sediment sizes include d_{50}, d_{65}, d_{84}, d_{90}, with units in feet, meters or millimeters. Very few relationships consider the rate of sediment transport as an independent parameter, and none expressed the sediment transport rate in terms of the Shields parameter.

The foregoing discussion proposes to: (1) compare the exponents of discharge and sediment size from empirical hydraulic geometry relationships with those obtained from (16)–(19); (2) examine the relative importance of the parameters m and p associated with the effects of relative submergence; and (3) discuss the qualitative effects of increasing discharge, sediment size, and sediment transport on the hydraulic geometry of alluvial channels. These three aspects are considered after plotting exponent diagrams showing the exponent of discharge as a function of the exponent of sediment size. Four exponent diagrams corresponding with each of the four hydraulic variables are shown in Figs. 4(a–d). On each diagram, the theoretical line is obtained from (16)–(19) with $0 < m < 0.5$, and $0 < p < 2m$.

The exponent diagram for flow depth h in Fig. 4(a) shows the theoretical relationship obtained from (16). Comparison with several empirical relationships found in the literature indicates a reasonable agreement between the theoretical values of the exponents and the empirical relationships for both sand-bed and gravel-bed channels. It is concluded that for flow depth the exponent of discharge decreases slightly, with relative roughness around a value close to 0.4, and the exponent of sediment size can either be negative or positive, with values roughly ranging from -0.3 to 0.3. Eq. (16) shows that flow depth is proportional to water discharge, and the negative exponent of the Shields parameter indicates that the flow depth varies inversely with sediment transport. These results are in agreement with the qualitative geomorphic principles for fluvial systems spelled out by Schumm (1977) and Simons et al. (1975). They suggested that $Q^+ \sim h^+$ and $Q_s^+ \sim h^-$, where the signs $^+$ and $^-$, denote an increase or decrease in the variable considered. The effect of sediment size is unclear and seems to depend on the value of relative roughness through the parameter m.

The exponent diagram for channel width W in Fig. 4(b) indicates that the exponent of the sediment size remains negative, with values between -0.4 and 0; and the exponent of discharge remains very close to 0.5, which is in remarkable agreement with the regime relationships proposed by Lacey (1929). From a theoretical standpoint, the values of both parameters m and p do not affect the exponent of discharge significantly. On the other hand, the exponent of sediment size is closer to zero when $p = 0$. It is concluded that the exponent of discharge remains close to 0.5 in all cases and the sediment size exponent varies around a value of -0.25, obtained when $p = m$. The small negative value of the exponent of the Shields parameter in (16) indicates that channel width is expected to decrease slightly with sediment transport.

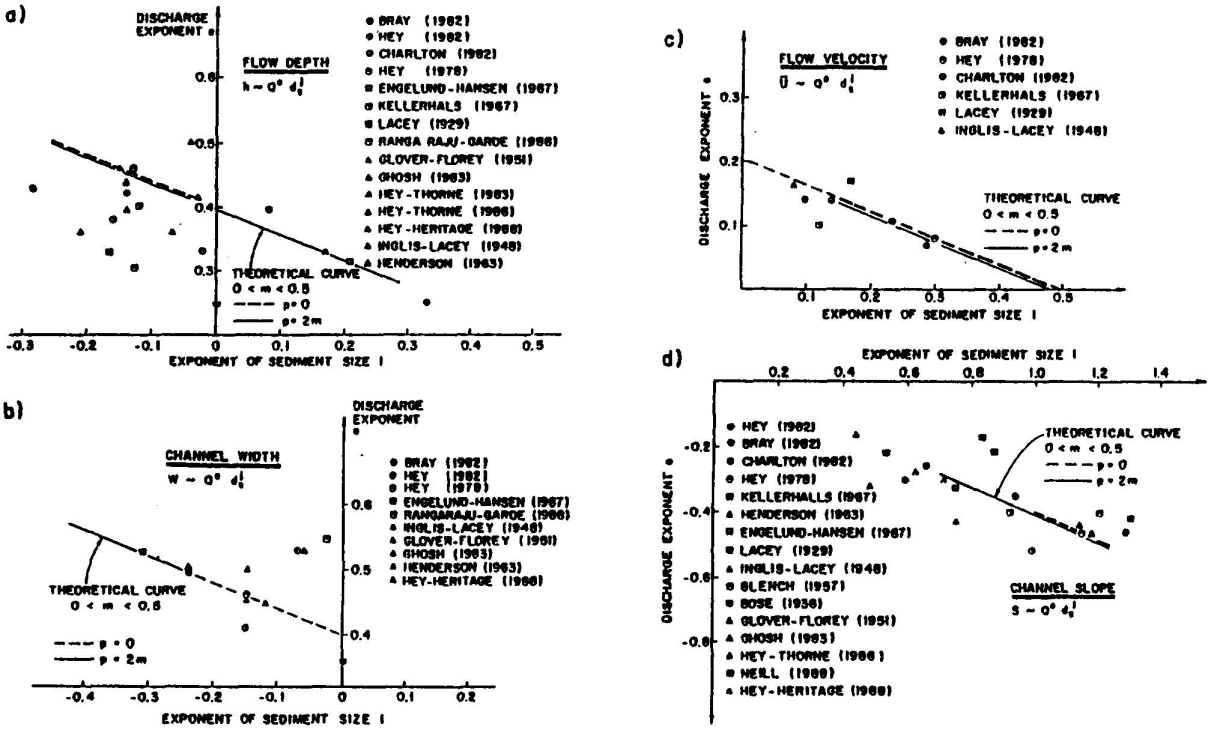

FIG. 4. Exponent diagram for: (a) Flow Depth; (b) Channel Width; (c) Flow Velocity; (d) Slope

The exponent diagram for flow velocity V shown in Fig. 4(c) indicates positive values for exponents of both discharge and sediment size. The exponent of discharge is less than 0.2 and the exponent of sediment size is less than 0.5. Both exponents are relatively small and the slight empirical decrease in the exponent of discharge as the exponent of sediment size increases is theoretically confirmed from (18). Eq. (18) also supports the geomorphic relations from Simons et al. (1975), in that $Q^+ \sim V^{\pm}$, $Q_s^+ \sim V^+$ and $d_s^+ \sim V^+$. The uncertain change in flow depth, from increasing discharge, results from the low values of the exponent of discharge [as given from (18) and shown in Fig. 4(c)].

The exponent diagram for the channel slope S in Fig. 4(d) is interesting in terms of the relatively large values of the exponents for discharge and sediment size. The exponent of sediment size ranges from 0.4 to 1.3, and the exponent of discharge remains negative from -0.2 to -0.6. The empirical relationships are well supported with the theoretical relationship (19). The slope is proportional to sediment size and rate of sediment transport but varies inversely with discharge. Once again, (19) supports the qualitative geomorphic principles ($Q^+ \sim S^-$; $d_s^+ \sim S^+$; and $Q_s^+ \sim S^+$) found by Simons et al. (1975) and Schumm (1977). The effects of changing sediment size and sediment transport are expected to be particularly significant because the exponents of both parameters are relatively large in (19).

QUANTITATIVE ANALYSIS

Field Data Set

The downstream hydraulic geometry measurements from 835 field channels and 45 laboratory channels were compiled by Wargadalam (1993) to test the four downstream hydraulic geometry relationships (16)–(19).

Church and Rood (1983) published a compendium of alluvial river regime data including 496 field hydraulic geometry measurements from an extensive search of the published literature. These relatively complete measurements from rivers in Canada and the United States were carefully selected from 25 references published between 1955–1983. In addition to this compendium, Hey and Thorne (1986) presented 62 river measurements from stable gravel-bed rivers in the United Kingdom. Griffiths (1981) collected 136 gravel-bed river geometry measurements from 46 rivers in New Zealand. From this data set, 84 measurements pertain to rigid bed and 52 reflect mobile bed conditions. Higginson and Johnston (1988) compiled 68 bank-full river conditions from rivers in North Ireland. Colosimo et al. (1988) collected gravel-bed river data in Calabria, southern Italy. Brownlie (1981) released an extensive compilation of laboratory and field data from which 28 different sets of sand-bed measurements were selected for the analysis. Khan (1971) presented 42 laboratory measurements of hydraulic geometry for straight, meandering, and braided sand-bed channels. Lan (1990) provided three additional laboratory channel measurements for meandering sand-bed channels.

The databases from Church and Rood (1983), Hey and Thorne (1983), Griffiths (1981), and Higginson and Johnston (1988) total 764 field data sets. This database was sorted according to increasing values of the relative submergence h/d_s, and was split into two subdata sets for the analysis. The first subset, called river data A, includes 382 measurements used to calibrate the hydraulic geometry relationships. The second subset, called river data B, also includes 382 measurements used to verify the hydraulic geometry relationships. Finally, a third data set combining a wide range of hydraulic geometry conditions is used for the independent validation of the regime equations. This third data set combines the gravel-bed river data of Colosimo, the sand-bed river data compiled by Brownlie (1981), and the laboratory channels of Khan (1971) and Lan (1990) for meandering and braided sand-bed channels. This third data set includes 115 measurements under very diversified conditions from sand to gravel beds, and from small laboratory channels to very large rivers, including meandering to braided channels.

The range of hydraulic and sediment conditions for each data set is compiled in Table 1. The discharge Q is in cubic meters per second (m^3/s), the top width W and average flow depth h are both in meters (m), the cross-section average velocity $\bar{U}$ is in meters per second (m/s), the median grain size d_{50} of the surface bed material is in meters, the friction slope S, the width-depth ratio W/h, the relative submergence h/d_{50}, the Froude number F, the Shields parameter τ_0^*, and the grain shear Reynolds number R_* are dimensionless parameters. In the data set, most discharge measurements refer to bank-full discharge; however, data points using mean annual discharge, and 2-yr flood and 5-yr flood discharge were included without correction in the analysis. Uncertainties in using different reference discharges contribute to the scatter in the final results. In this entire data set, the discharge varied from 0.00018 to 26,560 m^3/s. Thus, eight orders of magnitude separate discharges in large rivers from laboratory conditions. Likewise, grain sizes vary by three orders of magnitude, and the Shields parameter τ_0^* varies by almost four orders of magnitude. Some low values of the Shields parameter, below the threshold of motion, represent paved gravel-bed rivers, while large values of the Shields parameter indicate high rates of sediment transport in sand-bed channels. The relatively high values of the grain shear Reynolds number R_* indicate that the data set is representative of hydraulically rough

TABLE 1. Variability of Hydraulic and Sediment Parameters

Variables (1)	River A data (2)	River B data (3)	Colosimo data (4)	Brownlie data (5)	Laboratory data (6)
Number	382	382	42	28	45
Q^a	0.05–16950	0.54–16700	0.40–17.90	0.65–26600	0.00018–0.0085
W^b	2.00–900	2.0–832	3.0–23.00	3.92–1100	0.16–1.74
h^b	0.04–13.9	0.10–11.3	0.26–0.58	0.15–15.67	0.003–0.046
$\bar{U}^c$	0.09–4.4	0.23–4.70	0.43–2.71	0.67–2.93	0.11–0.73
S	0.00004–0.081	0.00004–0.075	0.0026–0.019	0.00004–0.00275	0.001–0.020
$d_{50}^b \times 10^{-3}$	0.15–400	0.12–265	20.5–60.00	0.188–1.44	0.13–0.70
W/h	5.24–420	4.163–282	10.26–52.9	9.94–280	5.6–507
h/d_{50}	1.42–44900	1.53–50800	4.50–24	152.0–70400	4.8–65
F	0.0167–1.72	0.082–1.74	0.269–1.26	0.116–0.98	0.40–4.0
τ^*	0.0011–8.50	0.00091–7.2	0.0203–0.103	0.15–6.28	0.02–0.30
R*	6.60–156000	7.32–71100	2030–14500	10.7–122000	1.60–30.0

[a]In cubic meters per second (m^3/s).
[b]In meters (m).
[c]In meters per second (m/s).

boundary conditions for which grain roughness can be determined by a logarithmic function of the relative submergence, as described by (2). Only the laboratory data set used for the validation seems to overlap the transition range to the hydraulically smooth surface.

Calibration of Regime Equations

The set of theoretical equations defining the hydraulic geometry of alluvial channels has been prescribed in (16)–(19). In the light of the extensive variability in Q, d_s, and τ_θ^*, the variability in the remaining five parameters R_w, b_r, ρ^*, α, and λ is considered to be comparatively small. These five parameters in the hydraulic geometry equations (16)–(19) are grouped to define four coefficients C_h, C_W, $C_{\bar{U}}$, and C_S, evaluated from measured values of Q, d_s, τ_θ^*, h, W, $\bar{U}$, and S

$$C_h = \frac{h}{Q^{1/(2+m+p)} d_s^{(-1+2m+2p)/(4+2m+2p)} \tau_\theta^{*\,-1/(4+2m+2p)}} = \alpha^{1/(2+m+p)} (\tan\lambda)^{1/(2+m+p)} \tag{20}$$

$$C_W = \frac{W}{Q^{(1+p)/(2+m+p)} d_s^{(-1+2m-3p)/(4+2m+2p)} \tau_\theta^{*(-1-p)/(4+2m+2p)}}$$

$$= \frac{b_r}{R_w} \alpha^{(1+p)/(2+m+p)} (\tan\lambda)^{(-1-m)/(2+m+p)} \tag{21}$$

$$C_{\bar{U}} = \frac{\bar{U}}{Q^{m/(2+m+p)} d_s^{(2-4m+p)/(4+2m+2p)} \tau_\theta^{*(2+p/(4+2m+2p)}} = \frac{R_w}{b_r} \alpha^{(-2-p)/(2+m+p)} (\tan\lambda)^{m/(2+m+p)} \tag{22}$$

$$C_S = \frac{S}{Q^{-1/(2+m+p)} d_s^{5/(4+2m+2p)} \tau_\theta^{*(5+2m+2p)/(4+2m+2p)}} = \rho^* \alpha^{-1/(2+m+p)} (\tan\lambda)^{-1/(2+m+p)} \tag{23}$$

Wargadalam (1993) conducted a thorough investigation of the effect of the exponent p on the calculated coefficient C_h, C_W, $C_{\bar{U}}$, and C_S. Three values of p were selected ($p = 2m$, $p = m$, $p = 0$), and the results were only slightly different in each case. Through statistical tests using river data A, the value $p = 2m$ minimized the variability of the four coefficients; thus, $p = 2m$ was selected for the remainder of the analysis.

The values of the four coefficients C_h, C_W, $C_{\bar{U}}$, and C_S for the 382 measurements from river data A with $p = 2m$ are plotted versus the relative submergence on Figs. 5(a–d). All the measurements center around the average value, without significant bias at large values of the relative submergence h/d_s. The average values of each parameter are the following: $\bar{C}_h = 0.133$, $\bar{C}_W = 0.512$, $\bar{C}_{\bar{U}} = 14.7$, and $\bar{C}_S = 12.4$. The dispersion of the data around the mean value is acceptable given that the coefficient of variation is between 0.4 and 0.5 for each of the four coefficients. Most important is that there is no systematic bias with relative submergence. Therefore, one should expect the observed values to range within a factor of 2; i.e., between 50% and 200% of the calculated values of the equilibrium depth, width, velocity, and slope.

The proposed simplified regime equations from $\bar{C}_h$, $\bar{C}_W$, $\bar{C}_{\bar{U}}$, and $\bar{C}_S$, and $p = 2m$ in (20)–(23) describe the equilibrium downstream hydraulic geometry of noncohesive alluvial channels in terms of average flow depth h (in m), surface width W (in m), average flow velocity $\bar{U}$ (in m/s), and friction slope S

$$h = 0.133 Q^{1/(3m+2)} d_s^{(6m-1)/(6m+4)} \tau_\theta^{*\,-1/(6m+4)} \tag{24}$$

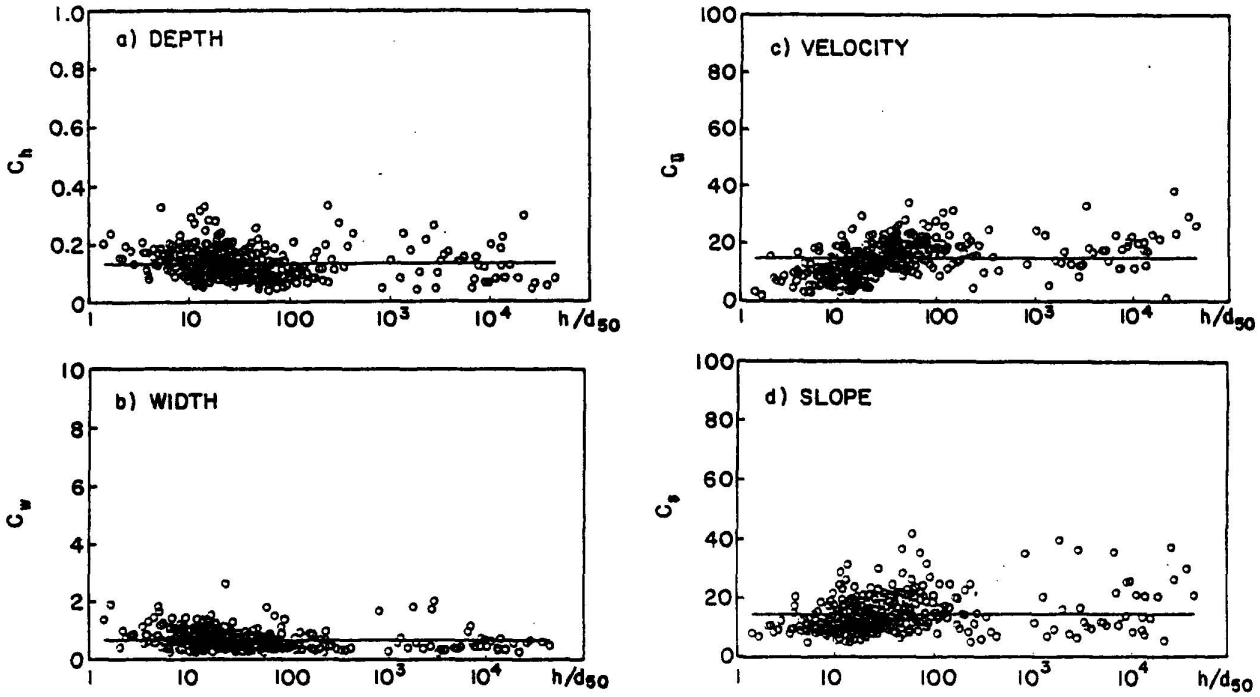

FIG. 5. Calibration of Coefficients: (a) C_h; (b) C_w; (c) C_U; (d) C_s

$$W = 0.512Q^{(2m+1)/(3m+2)}d_s^{(-4m-1)/(6m+4)}\tau_\theta^{*(-2m-1)/(6m+4)} \tag{25}$$

$$\bar{U} = 14.7Q^{m/(3m+2)}d_s^{(2-2m)/(6m+4)}\tau_\theta^{*(2m+2)/(6m+4)} \tag{26}$$

$$S = 12.4Q^{-1/(3m+2)}d_s^{5/(6m+4)}\tau_\theta^{*(6m+5)/(6m+4)} \tag{27}$$

from the equilibrium or dominant flow discharge Q (in m^3/s), the median grain size $d_s = d_{50}$ in meters, and the Shields parameter $\tau_\theta^* = K\gamma hS/(\gamma_s - \gamma)\, d_{50}$, given the resistance exponent m calculated from $m = 1/\ln(12.2\, h/d_{50})$.

Verification and Validation with Observed Data

The verification of the proposed equations consisted of applying the proposed regime equations (24)–(27) to river data set B with 382 measurements. River data set B did not serve for the calibration of the four coefficients. The results are plotted in Figs. 6(a–d) for the values of flow depth, surface width, average flow velocity, and slope, respectively. The agreement is considered to be very good, with about 95% of the calculated parameters within 50% and 200% of the field measurements.

The difficult task of predicting the hydraulic geometry of a widely varied data set has been imposed to validate the proposed regime equations. The data set includes 115 measurements for both sand-bed and gravel-bed channels, channel widths ranging from 0.1 to 1,000 m, from both meandering and braided streams on very flat to steep slopes. The gravel-bed river data set of Colosimo et al. (1988) consists of 42 observations, with grain sizes up to 60 mm. A sample of 28 different sand-bed river reaches has been selected from Brownlie's (1981) database. Finally, 45 laboratory channels from Khan (1971) and Lan (1990) are representative of very small sand-bed channels on steep slopes; moreover, the data covers the transition range between hydraulically rough and hydraulically smooth boundaries.

The validation results are shown in Figs. 7(a–d). All calculations for gravel-bed rivers are in very good agreement with field observations. For sand-bed channels, the calculated velocity and slope are slightly lower than the observations. The agreement is also very good for laboratory channels, while the calculated flow depth tends to overpredict flow depth measurements. Most observations remain within 50% and 200% of the calculations. The overall agreement is acceptable, considering that the flow depth and channel width vary by four orders of magnitude.

CALCULATION PROCEDURE

The equilibrium downstream hydraulic geometry of noncohesive alluvial channels can be calculated given the dominant discharge Q (in m^3/s), the median grain size d_{50} (in m), and the

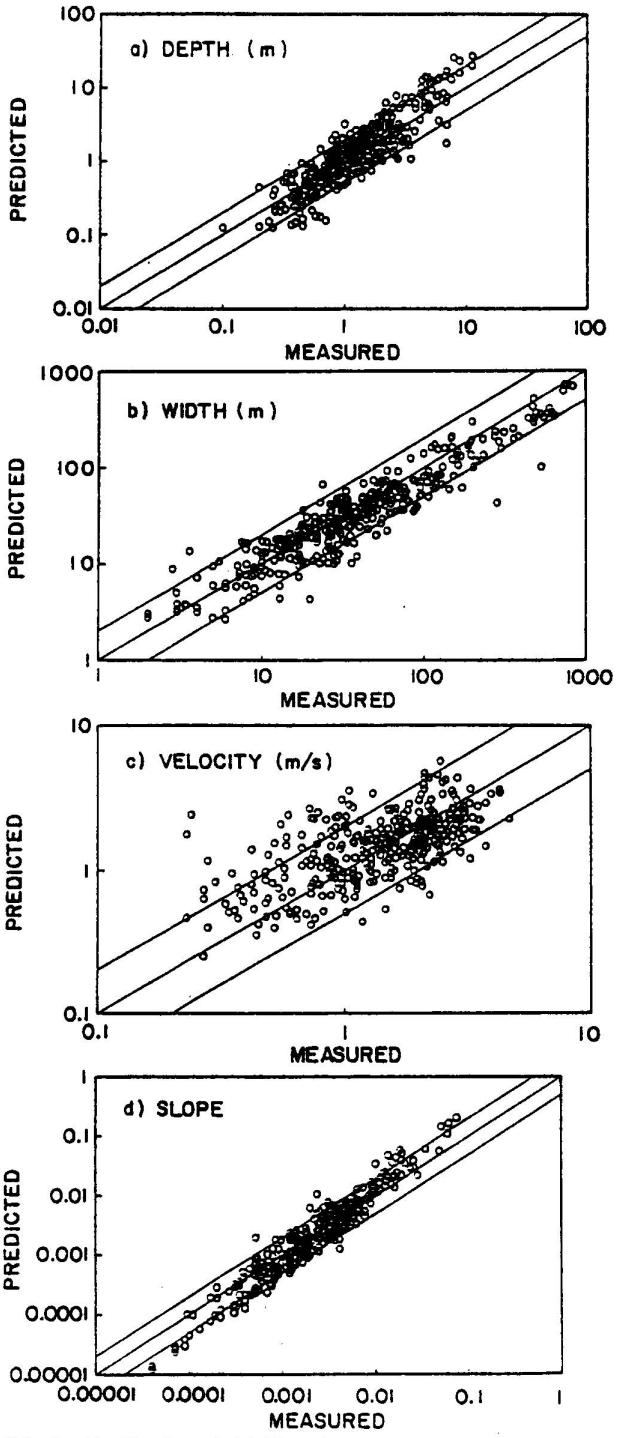

FIG. 6. Verification of: (a) Flow Depth; (b) Channel Width; (c) Flow Velocity; (d) Slope

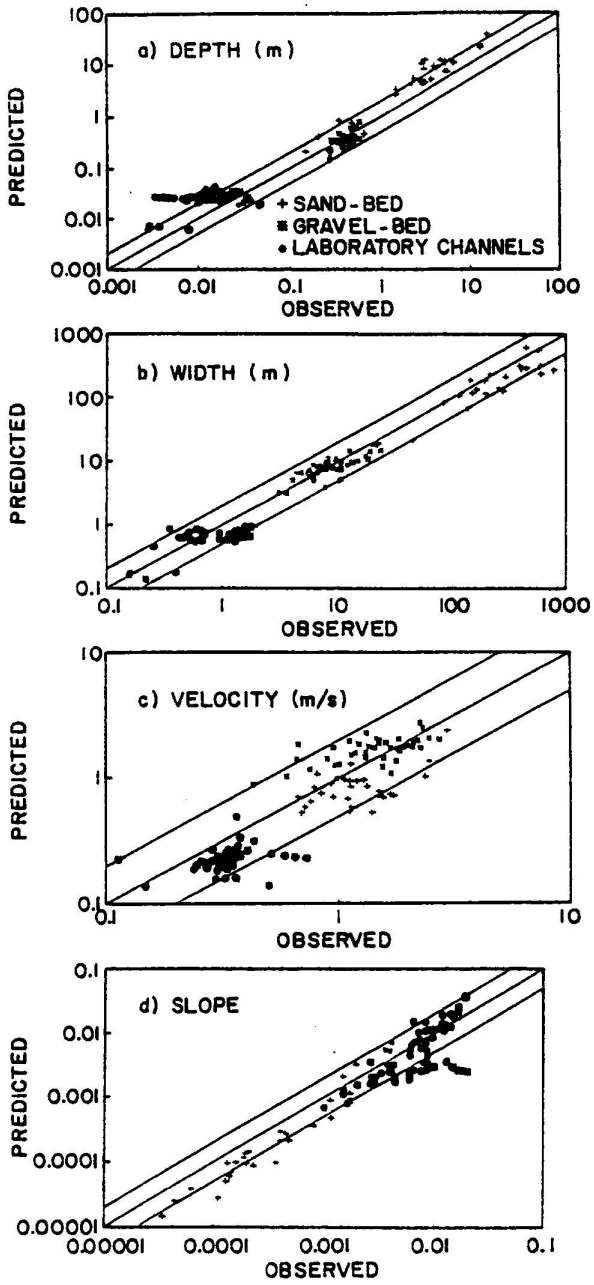

FIG. 7. Validation of: (a) Flow Depth; (b) Channel Width; (c) Flow Velocity; (d) Slope

dimensionless Shields parameter τ_0^*. The calculation procedure is illustrated with the following example of a gravel-bed channel, $d_{50} = 0.056$ m near incipient motion τ_0^*, at a bank-full discharge of 104 m^3/s. Because the exponents of the regime equations (24)–(27) are not constant, the following simple iterative procedure is proposed:

1. Roughly estimate the flow depth; e.g., $h = 1$ m.
2. From the flow depth and grain size, calculate the parameter m from $m = 1/\ln(12.2\ h/d_s)$; e.g., $m = 0.186$.

3. Substitute the values of Q, d_{50}, τ_θ^*, and m into (24) to calculate the flow depth; e.g., $h = 0.133\ (104)^{0.39}(0.056)^{0.023}(0.047)^{-0.195} = 1.38$ m.
4. Repeat steps 2 and 3 with the calculated flow depth until convergence; e.g., $m = 0.175$, $h = 1.49$ m and $m = 0.172$, $h = 1.51$ m.
5. Calculate the channel width (25), flow velocity (26), and slope (27) using the last value of m; e.g., with $m = 0.172$; $W = 0.512\ (104)^{0.534}\ (0.056)^{-0.335}\ (0.047)^{-0.267} = 36.4$ m, $V = 1.9$ m/s and $S = 2.87 \times 10^{-3}$.

Should the value of the Shields parameter be unknown, the hydraulic geometry of a stable channel design can be calculated after assuming the threshold of motion of bed material $\tau_\theta^* = 0.047$. This is a reasonable first approximation for gravel-bed rivers, e.g., Andrews (1984). The effect of sediment transport on the hydraulic geometry of the channel can be simulated by increasing the Shields parameter beyond this critical value. For instance, the effect of high sediment transport rates in sand-bed channels can be estimated by using $\tau_\theta^* = 1$ in (24)–(27). With increasing sediment transport, the channel width and depth are slightly reduced and the velocity and slope increase largely.

Finally, should the field slope be available, the Shields parameter can be calculated from (12) and (6) after the flow depth calculation from (24). Alternatively, the hydraulic geometry relationships can be rewritten to express the dependent variables h, W, $\tilde{U}$, and τ_θ^* as a function of the independent variables Q, d_s, and S:

$$h = 0.2Q^{2/(5+6m)}d_s^{6m/(5+6m)}S^{-1/(5+6m)} \tag{28}$$

$$W = 1.33Q^{(2+4m)/(5+6m)}d_s^{-4m/(5+6m)}S^{-(1+2m)/5+6m} \tag{29}$$

$$\tilde{U} = 3.76Q^{(1+2m)/5+6m}d_s^{-2m(5+6m)}S^{(2+2m)/(5+6m)} \tag{30}$$

$$\tau_\theta^* = 0.121Q^{2/(5+6m)}d_s^{-5/(5+6m)}S^{(4+6m)/(5+6m)} \tag{31}$$

The reader is referred to Wargadalam (1993) for the calibration, verification, and validation of (28)–(31). The agreement with field observations is comparable with (24)–(27) shown in Figs. 4–7. The calculation procedure to solve (28)–(31) is similar to the procedure required to solve (24)–(27).

SUMMARY AND CONCLUSIONS

The downstream hydraulic geometry of alluvial channels is examined from a 3D stability analysis of noncohesive particles under 2D flows. Four governing equations are identified to define hydraulic geometry: flow rate, resistance to flow, secondary flow, and particle mobility. The governing equations can be solved to analytically define the downstream hydraulic geometry of noncohesive alluvial channels as a function of water discharge, sediment size, Shields number, and streamline deviation angle. Exponent diagrams are defined because the exponents of hydraulic geometry relationships change with relative submergence h/d_s. When compared with empirical relationships available in the literature, the four exponent diagrams are in very good agreement with several empirical relationships for sand-bed and gravel-bed streams.

This analysis concludes that the hydraulic geometry of alluvial channels in terms of width, depth, velocity, and slope can be analytically defined by combining four governing equations. The proposed theoretical relationships (16)–(19) can satisfactorily explain and predict the behavior of the exponents of discharge and grain size in hydraulic geometry relationships incurred by changes in relative submergence, as shown in the four exponent diagrams [Figs. 4(a–d)].

The downstream hydraulic geometry equations (16)–(19) are then simplified after considering the variability of each parameter. The resulting regime equations (24)–(27) are quantitatively tested with an extensive data set consisting of 835 field channels and 45 laboratory channels for meandering and braided sand-bed and gravel-bed channels. The analysis consists of a calibration with 382 measurements of river data A, a verification of the calibrated relationships with 382 different measurements from river data B, followed by a validation of the same relationships with 115 diversified measurements from meandering and braided sand-bed and gravel-bed rivers and laboratory channels. The results shown in Figs. 6 and 7 reveal that each hydraulic geometry parameter can be calculated within 50% and 200% of the observations with the proposed regime equations (24)–(27). For practical applications, an iterative procedure is provided for the calculation of channel width, flow depth, mean flow velocity, and channel slope given the dominant discharge, the median grain size of the bed material, and the Shields parameter.

ACKNOWLEDGMENTS

This study was first conducted under the support of a NATO postdoctoral fellowship from the Natural Sciences and Engineering Research Council of Canada. Comparisons with field data were made possible by a USAID

grant to the second writer from the Overseas Training Office of the Government of Indonesia. Recent developments were completed at the Army Research Office (ARO)-supported Center for Geosciences at Colorado State University, under Grant ARO/DAAL 03-86-K-0175. The writers also appreciate the useful comments and constructive criticism received from Y. Q. Lan and anonymous reviewers.

APPENDIX I. REFERENCES

Ackers, P. (1964). "Experiments on small streams in alluvium." *J. Hydr. Div.*, ASCE, 90(4), 1–37.
Andrews, E. D. (1984). "Bed-material entrainment and hydraulic geometry of gravel-bed rivers in Colorado." *Bull. Geological Soc.*, Am. 95, 371–378.
Blench, T. (1969). *Mobile-bed fluviology, a regime treatment of canals and rivers.* Univ. of Alberta Press, Edmonton, Alberta, Canada.
Blench, T. (1957). *Regime behavior of canals and rivers.* Butterworth, London, England.
Blench, T. (1972). "Regime problems of rivers formed in sediment." *Environmental impact on rivers*, H. W. Shen, ed., Publisher, Ft. Collins, Colo.
Bose, N. K. (1936). "Silt movement and design of channels." *Proc., Punjab Engrg. Congr.* , Punjab, India, 192.
Bray, D. I. (1979). "Estimating average velocity in gravel-bed rivers." *J. Hydr. Div.*, ASCE, 105(9), 1103–1122.
Bray, D. I. (1982). "Flow resistance in gravel-bed rivers." *Gravel-bed rivers*, John Wiley & Sons, Inc., New York, N.Y., 109–137.
Brownlie, W. R. (1981). "Prediction of flow depth and sediment discharge in open channels," PhD dissertation, California Inst. of Technol., Pasadena, Calif.
Callander, R. A. (1978). "River meandering." *Annu. Rev. of Fluid Mech.*, 10, 129–158.
Charlton, F. G. (1982). "River stabilization and training in gravel-bed rivers." *Gravel-bed rivers*, John Wiley & Sons, Inc., 635–657.
Charlton, F. G., Brown, P. M., and Benson, R. W. (1978). "The hydraulic geometry of some gravel rivers in Britain." *Rep. IT 180*, Hydr. Res. Station, Wallingford, England.
Chien, N. (1957). "A concept of the regime theory." *Trans., ASCE*, 122, 785–793.
Chitale, S. V. (1973). "Theory and relationship of river channel patterns." *J. Hydrol.*, Vol. 19, 285–308.
Church, M., and Rood, R. (1983). "Catalogue of alluvial river channel regime data." *Rep.*, Dept. of Geography, Univ. of British Columbia, Vancouver, Canada.
Colosimo, C., Coppertino, V. A., and Veltri, M. (1988). "Friction factor evaluation in gravel-bed rivers." *J. Hydr. Engrg.*, ASCE, 114(8), 861–876.
de Vriend, H. J. (1977). "A mathematical model of steady flow in curved shallow channels." *J. Hyd. Res.*, 15(1), 37–53.
Dietrich, W. E., and Smith, J. D. (1984). "Bed load transport in a river meander." *Water Resour. Res.*, 20(10), 1355–1380.
Einstein, H. A., and Chien, N. (1954). "Similarity of distorted river models with unstable beds." *Proc., ASCE*, 80(566).
Engelund, F. (1974). "Hydraulic resistance of alluvial streams." *J. Hydr. Div.*, 93(4), 287–296.
Engelund, F., and Skovgaard, O. (1973). "On the origin of meandering and braiding in alluvial streams." *J. Fluid Mech.*, 57(Part 2), 289–302.
Engelund, F., and Hansen, F. (1967). "A monograph on sediment transport in alluvial streams." *Monograph*, Teknisk Forlag, Copenhagen, Denmark.
Engelund, F., and Fredsoe, J. (1982). "Hydraulic theory of alluvial rivers." *Advances in hydroscience*, 13, Academic Press, Inc., San Diego, Calif., 187–215.
Fredsoe, J. (1978). "Meandering and braiding of rivers." *J. Fluid Mech.*, 84(Part 4), 609–624.
Ghosh, S. K. (1983). "A study of regime theories for an alluvial meandering channel." *Proc., 2nd Int. Symp. on River Sedimentation*, China Ocean Press, Beijing, China, Vol. 1, 706–712.
Gill, M. A. (1968). "Rationalization of Lacey's regime flow equations." *J. Hydr. Div.*, ASCE, 94(4), 983–995.
Glover, R. E., and Florey, Q. L. (1951). "Stable channel profiles." *Rep. Hyd-325*, U.S. Bureau Reclamation, Hydr. Lab., U.S. Dept. of Interior, Des. and Constr. Div., Denver, Colo.
Griffiths, G. A. (1981). "Stable channel design in gravel-bed rivers." *J. Hydrol.*, 52(3/4), 291–305.
Henderson, F. M. (1961). "Stability of alluvial channels." *J. Hydr. Div.*, 87(6), 109–138.
Henderson, F. M. (1963). "Stability of alluvial channels." *Trans., ASCE*, 128(3440), 657–686.
Henderson, F. M. (1966). *Open channel flow.* MacMillan, New York, N.Y.
Hey, R. D. (1978). "Determinate hydraulic geometry of river channels." *J. Hydr. Div.*, 104(6), ASCE, 869–885.
Hey, R. D. (1982). "Design equations for mobile gravel-bed rivers." *Gravel-bed rivers*, John Wiley & Sons, Inc., New York, N.Y., 553–580.
Hey, R. D., and Heritage, G. L. (1988). "Dimensional and dimensionless regime equations for gravel-bed rivers." *Proc., Intl. Conf. River Regime*, John Wiley & Sons, Inc., New York, N.Y., 1–8.
Hey, R. D., and Thorne, C. R. (1983). "Hydraulic geometry of mobile gravel-bed rivers." *Proc., 2nd Intl. Symp. River Sedimentation*, China Ocean Press, Beijing, China, Vol. 1, 713–723.
Hey, R. D., and Thorne, C. R. (1986). "Stable channels with mobile gravel beds." *J. Hydr. Engrg.*, ASCE, 112(6), 671–689.
Higginson, N. N. J., and Johnston, H. T. (1988). "Estimation of friction factors in natural streams." *River regime*, John Wiley & Sons, Inc., New York, N.Y., 251–266.
Hussein, A. S., and Smith, K. V. H. (1986). "Flow and bed deviation angle in curved open channels." *J. Hydr. Res.*, 24(2), 93–108.
Ikeda, S., Parker, G., and Sawai, K. (1981). "Bend theory of river meanders. Part 1: linear development." *J. Fluid Mech.*, Vol. 112, 363–377.
Inglis, C. C. (1948). "Historical note on empirical equations developed by engineers in India for flow of water and sand in alluvial channels." *Proc., IAHR.*, Nat. Res. Council, Ottawa, Canada.
Julien, P. Y. (1988). "Downstream hydraulic geometry of noncohesive alluvial channels." *Int. Conf. on River Regime*, John Wiley & Sons, Inc., New York, N.Y., 9–16.
Julien, P. Y. (1989). "Geometrie hydraulique des cours d'eau a lit alluvial." *Proc., IAHR Conf.*, Nat. Res. Council, Ottawa, Canada, B9–16.

Kellerhals, R. (1967). "Stable channels with gravel-paved beds." *J. Watrwy. Div.*, ASCE, 93(1), 63–84.
Kennedy, R. G. (1895). "The prevention of silting in irrigation canals." *Proc., Inst. of Civ. Engrs.*, London, England, Vol. CXIX.
Keulegan, G. H. (1938). "Laws of turbulent flows in open channels." *J. Res. Nat. Bureau Standards*, 21(RP 1151), 707–741.
Khan, H. R. (1971). "Laboratory study of alluvial river morphology," PhD dissertation, Colorado State Univ., Fort Collins, Colo.
Lacey, G. (1929). "Stable channels in alluvium." *Proc., Inst. Civ. Engrs.*, London, England, Vol. 229.
Lan, Y. Q. (1990). "Dynamic modeling of meandering alluvial channels," PhD dissertation, Colorado State Univ., Fort Collins, Colo.
Lane, E. W. (1937). "Stable channels in erodible material." *Trans., ASCE*, Vol. 102.
Lane, E. W. (1955). "Design of stable channels." *Trans., ASCE*, Vol. 120, 1234–1279.
Leopold, L. B., and Maddock, T. (1953). "The hydraulic geometry of stream channels and some physiographic implications." *USGS Profl. paper 252*, U.S. Geological Survey, Washington, D.C.
Leopold, L. B., and Wolman, M. G. (1957). "River channel patterns: braided, meandering and straight." *USGS Profl. paper 282-B*, U.S. Geological Survey, Washington, D.C., 38–85.
Lindley, E. S. (1919). "Regime channels." *Proc., Punjab Engrg. Congr.*, Punjab, India., VII.
Mahmood, K., and Shen, H. W. (1971). "The regime concept of sediment-transporting canals and rivers." *River mechanics*, H. W. Shen, ed./publisher, Fort Collins, Colo., 30.
Mussetter, R. A. (1989). "Dynamics of mountain streams," PhD Dissertation, Dept. of Civ. Eng., Colorado State Univ., Ft. Collins, Colo.
Neill, C. R. (1988). "Discussion on 'Stable channels with mobile gravel-beds,' by Hey and Thorne,"*J. Hydr., Engrg.*, ASCE 114(3), 339–341.
Odgaard, A. J. (1981). "Transverse bed slope in alluvial channel bends." *J. Hydr. Div.*, ASCE, 107(12), 1677–1694.
Parker, G. (1976). "On the cause and characteristic scales of meandering and braiding in rivers." *J. Fluid Mech.*, Vol. 76, 457–480.
Parker, G. (1978a). "Self-formed straight rivers with equilibrium banks and mobile bed. Part 1: the sand-silt river." *J. Fluid Mech.*, Vol. 89, 109–126.
Parker, G. (1978b). "Self-formed straight rivers with equilibrium banks and mobile bed. Part 2: the gravel river." *J. Fluid Mech.*, Vol. 89, 127–146.
Ranga Raju, K. J., and Garde, K. J. (1988). "Design of stable canals in alluvial material." *Int. J. Sediment Res.*, 3(1), 10–37.
Rozovskii, I. L. (1961). *Flow of water in bends of open channels*. Translated by Y. Prushansky, Israel Program Sci. Translation, Jerusalem, Israel.
Schumm, S. A. (1977). *The fluvial system*. Wiley Interscience, New York, N.Y.
Simons, D. B., and Albertson, M. L. (1963). "Uniform water conveyance channels in alluvial material." *Trans., ASCE*, 128(1), 65–167.
Simons, D. B., Richardson, E. V., and Mahmood, K. (1975). "One-dimensional modeling of alluvial rivers." *Unsteady flow in open channels*, Water Resour. Publ., Littleton, Colo., 813–877.
Simons, D. B., and Senturk, F. (1977). *Sediment transport technology*. Water Resour. Publ., Littleton, Colo.
Stebbins, J. (1963). "The shapes of self-formed model alluvial channels." *Proc., Inst. Civ. Engrs.*, London, England, Vol. 25.
Stevens, M. A., and Simons, D. B. (1971). "Stability analysis for coarse granular material on slopes." *River mechanics*, H. W. Shen, ed./Publisher, Fort Collins, Colo.
Wargadalam, J. (1993). "Hydraulic geometry equations of alluvial channels," PhD dissertation, Colorado State Univ., Fort Collins, Colo.
Yalin, M. S. (1992). *River mechanics*, Pergamon Press, New York, N.Y.
Zimmermann, C. (1977). "Roughness effects on the flow direction near curved stream beds." *J. Hydr. Res.*, 15(1), 73–85.

APPENDIX II. NOTATION

The following symbols are used in this paper:

a = coefficient of logarithmic resistance equation;
a_1, a_2 = arbitrary exponents of sediment size;
b = coefficient of resistance equation;
b_r = coefficient of transversal resistance equation;
C = Chezy coefficient;
C_h, C_w, C_U, C_s = coefficients of regime equations;
c, d = moment arms of radial hydraulic forces;
D = coefficient of deviation angle equation;
d_{50}, d_{65}, d_{84}, d_{90}, d_s = sediment sizes for which 50%, 65%, 84%, and 90%, respectively, of material by weight is finer, sediment size;
e = exponent of discharge;
F_b = buoyancy force;
F_c = centrifugal force;
F_d = drag force;
F_l = lift force;
F_p = pressure force;
F_s = shear force;
F = Froude number;
f = Darcy-Weisbach friction factor;

g = gravitation acceleration;
h = average flow depth;
i = exponent of sediment size;
K = coefficient in depth-hydraulic radius relationship;
m = exponent of resistance equation;
p = transversal resistance exponent;
Q = dominant discharge;
R = reference radius of curvature;
R^* = grain shear Reynolds number;
R_A = reference point;
R_h = hydraulic radius;
R_w = ratio of radius of curvature to channel width;
r = local radius of curvature;
S = channel slope;
S_r = radial water surface slope;
S_{RA} = reference radial water surface slope;
s = downstream local coordinate;
$\bar{U}$ = average flow velocity;
u = local downstream velocity;
W = channel width;
W_p = weight of a particle;
W_s = submerged weight of a particle;
w = local horizontal coordinate;
z = local vertical coordinate;
$\forall$ = volume of fluid;
α = hydraulic geometry parameter;
β = particle motion angle;
η' = modified Shields number;
θ = embankment slope;
κ = von Kármán constant;
λ = flow deviation angle;
ρ = mass density of fluid;
ρ_s = mass density of sediments;
$\rho^* = (\rho_s - \rho)/\rho K$ = dimensionless submerged density of sediment;
τ_r = local radial shear stress;
τ_{rR} = reference radial shear stress;
τ_θ = downstream bed shear stress;
τ_θ^* = Shields number;
$\tau_{\theta c}^*$ = critical Shields number;
ϕ = angle of repose;
Ψ = particle stability factor;
Ψ_λ = relative particle stability factor; and
Ω_r = ratio of centrifugal to shear forces.

Superscripts

$+$ = increase in parameter value;
$-$ = decrease in parameter value; and
$*$ = dimensionless parameter.